

# Dielectric properties of electron-beam deposited Ga<sub>2</sub>O<sub>3</sub> films

M. Passlack, N. E. J. Hunt, E. F. Schubert, G. J. Zydzik, M. Hong, J. P. Mannaerts, R. L. Opila, and R. J. Fischer  
AT&T Bell Laboratories, Murray Hill, New Jersey 07974

(Received 16 December 1993; accepted for publication 27 February 1994)

We have fabricated high quality, dielectric Ga<sub>2</sub>O<sub>3</sub> thin films. The films with thicknesses between 40 and 4000 Å were deposited by electron-beam evaporation using a single-crystal high purity Gd<sub>3</sub>Ga<sub>5</sub>O<sub>12</sub> source. Metal-insulator-semiconductor (MIS) and metal-insulator-metal structures (MIM) were fabricated in order to determine dielectric properties, which were found to depend strongly on deposition conditions such as substrate temperature and oxygen pressure. We obtained excellent dielectric properties for films deposited at substrate temperatures of 40 °C with no excess oxygen and at 125 °C with an oxygen partial pressure of  $2 \times 10^{-4}$  Torr. Specific resistivities  $\rho$  and dc breakdown fields  $E_m$  of up to  $6 \times 10^{13}$  Ω cm and 2.1 MV/cm, respectively, were measured. Static dielectric constants between 9.93 and 10.2 were determined for these films. Like in other dielectrics, the current transport mechanisms are found to be bulk rather than electrode controlled.

Gallium oxide has proven to be a useful material for many applications including metal-insulator-structures on GaAs,<sup>1</sup> and facet coatings for GaAs based lasers.<sup>2</sup> Gallium oxide has also been used in oxygen sensors operating at high temperatures.<sup>3</sup> Stringent electrical and/or optical requirements have to be met including (i) low density of states below or in the  $10^{11}$  cm<sup>-2</sup> eV<sup>-1</sup> range located in the forbidden gap at the insulator-semiconductor interface, (ii) very good dielectric properties, and (iii) an index of refraction close to  $\sqrt{n_{\text{GaAs}}}$ , which gives  $n \approx 1.88^4$  for a 0.98 μm laser.

It has been demonstrated, that gallium oxide meets both requirements of refractive index and low density of interface states. The refractive index of bulk Ga<sub>2</sub>O<sub>3</sub> is between 1.9 and 1.92.<sup>5</sup> We report on optical properties including indices of refraction between 1.80 and 1.91 for thin Ga<sub>2</sub>O<sub>3</sub> films in another paper,<sup>2</sup> which demonstrates Ga<sub>2</sub>O<sub>3</sub> coatings on laser facets. Callegari *et al.*<sup>1</sup> showed that gallium oxide, in conjunction with a GaAs surface previously treated *in situ* by H<sub>2</sub> and N<sub>2</sub> plasma, gives insulator-semiconductor interfaces with a very low density of states. An electrical characterization of the gallium oxide-GaAs interface by capacitance-voltage (C-V) measurements at 1 MHz showed almost no stretching out of C-V curves. This indicates a midgap interface state density well below  $10^{11}$  cm<sup>-2</sup> eV<sup>-1</sup>, which is the detection limit of Terman's method.<sup>6</sup> Furthermore, *in situ* photoluminescence and Fourier transform infrared spectroscopy measurements revealed growth of Ga<sub>2</sub>O<sub>3</sub> on a GaAs surface during passivation of surface states in a NH<sub>3</sub> or H<sub>2</sub> plasma at room temperature.<sup>7</sup>

Ga<sub>2</sub>O<sub>3</sub> was fabricated in different ways,<sup>8</sup> however, excellent dielectric properties of thin films have not been reported yet. So far, gallium oxide films were deposited by electron-beam evaporation of Ga in an O<sub>2</sub> radio frequency plasma.<sup>1</sup> These films, however, show poor dielectric properties and are not practical for MIS structures and laser facet coatings.

We have developed a new method of depositing homogeneous, high quality dielectric Ga<sub>2</sub>O<sub>3</sub> films. Our single-crystal high purity (99.999%) Gd<sub>3</sub>Ga<sub>5</sub>O<sub>12</sub> source combines the relatively covalent oxide Ga<sub>2</sub>O<sub>3</sub>, which volatilizes near 2000 K, and the pretransition oxide Gd<sub>2</sub>O<sub>3</sub> which has a boil-

ing point (>4000 K) well above the foregoing temperature. The more complex compound Gd<sub>3</sub>Ga<sub>5</sub>O<sub>12</sub> (melting point ≈2000 K) decrepitates during heating, *slowly* releasing high purity Ga<sub>2</sub>O<sub>3</sub>.<sup>9</sup> Using this method, we have deposited homogeneous, high quality dielectric Ga<sub>2</sub>O<sub>3</sub> films with thicknesses between 40 and 4000 Å. The substrates were held at temperatures  $T_s$  between 40 and 370 °C during deposition and we investigated both cases of no excess oxygen and bleeding in of additional O<sub>2</sub> into the evaporation chamber to prevent reduction of films which may occur at higher deposition temperatures.<sup>9</sup> The background pressure in the chamber (no bleeding in of O<sub>2</sub>) was at  $1-2 \times 10^{-6}$  Torr. The maximum partial O<sub>2</sub> pressure was  $2 \times 10^{-4}$  Torr. The deposition rate, which was held at 0.5 Å/s, and the film thickness were measured during deposition by a crystal thickness monitor.

The films were deposited on Si wafers covered by a 900 Å thick TiW metal layer and on n<sup>+</sup> GaAs substrates. All films show an excellent homogeneity as demonstrated by Auger depth profiling. Figure 1 shows the depth profile of a

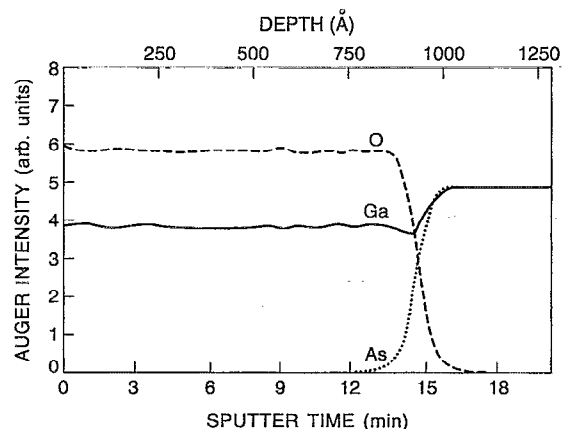


FIG. 1. Auger depth profile of a 955 Å thick Ga<sub>2</sub>O<sub>3</sub> layer deposited at 125 °C with O<sub>2</sub> partial pressure of  $2 \times 10^{-4}$  Torr. The analysis was done by using 4 keV Ar ions and the sensitivity factors for Ga and O were calibrated against pressed Ga<sub>2</sub>O<sub>3</sub> powder. The nominal etch rate is 65 Å/min. The film is homogeneous and stoichiometric.

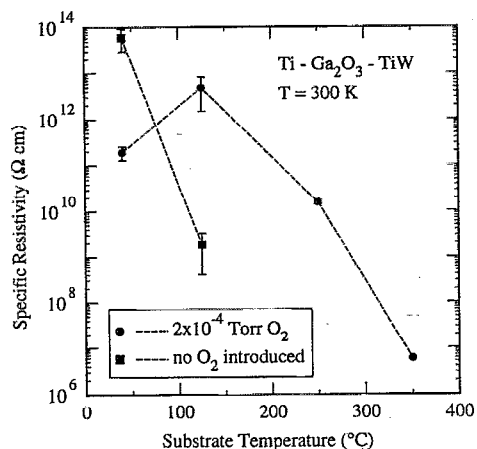


FIG. 2. Specific resistivities as a function of substrate temperature. Results are shown for the limits of no excess oxygen and  $2 \times 10^{-4}$  Torr oxygen present in the evaporation chamber. About ten films with thicknesses between 40 and 4000 Å were measured for each data point. The resistivity was determined at low fields ( $< 50$  kV/cm). Lines are guides to the eye.

955 Å thick  $\text{Ga}_2\text{O}_3$  layer deposited at 125 °C at an  $\text{O}_2$  partial pressure of  $2 \times 10^{-4}$  Torr. The measurements also demonstrate that, within the limits of Auger spectroscopy, the films are stoichiometric. No impurities could be detected by Auger analysis (sensitivity  $\geq 0.1\%$ ) including Gd, which is considered to be the dominant impurity in our  $\text{Ga}_2\text{O}_3$  films. The Gd content estimated by SIMS was of the order of 0.1%.

MIS and MIM structures were fabricated by evaporating Ti/Au dots of different diameters (50, 100, 200, and 500  $\mu\text{m}$ ) through a shadow mask. Capacitance-voltage ( $C$ - $V$ ) characteristics were recorded on an HP 9194 A impedance/gain-phase analyzer. Current-voltage ( $I$ - $V$ ) measurements were made using an HP 4145A parameter analyzer and an HP 4140B pA meter. The thicknesses of the deposited films were measured by ellipsometry at both 633 and 840 nm wavelength in order that the static dielectric constant  $\epsilon_s$ , specific resistivity  $\rho$ , and dc breakdown field  $E_m$  could be determined. All properties described in the following were obtained for as-deposited films. No annealing procedures have been carried out.

Specific resistivities and breakdown fields were determined for a large range of deposition conditions. Both quantities vary strongly with substrate temperature,  $\text{O}_2$  partial pressure, and position of the oxygen leak in the chamber. If  $\text{O}_2$  was introduced, the best results were obtained by positioning the oxygen leak valve close to the crucible. Figure 2 shows measured specific resistivities as a function of substrate temperature for the limits of no excess oxygen and  $2 \times 10^{-4}$  Torr oxygen present in the evaporation chamber. The resistivity  $\rho$  was determined from  $I$ - $V$  measurements of MIM structures at low fields ( $< 50$  kV/cm).  $\rho$  varies by almost 8 orders of magnitude dependent on deposition conditions, and is especially sensitive to substrate temperature for deposition without excess  $\text{O}_2$ . The best results of  $\rho = (6 \pm 3) \times 10^{13}$   $\Omega$  cm were obtained for  $T_s = 40$  °C with no introduction of oxygen. A relatively small change in substrate temperature from 40 to 125 °C, however, leads to a

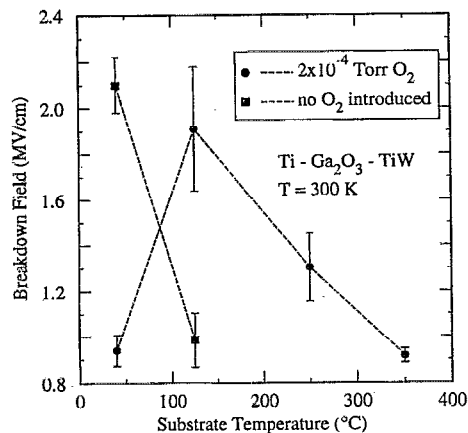


FIG. 3. dc breakdown field vs substrate temperature for the experimental limits of  $\text{O}_2$  partial pressure. About ten films with thicknesses between 500 and 4000 Å were measured for each data point. The breakdown voltage was determined by applying a voltage ramp between 0.1 and 0.3 V/s until thermal breakdown occurred. Lines are guides to the eye.

drastically reduced  $\rho$  of  $(2 \pm 1) \times 10^9$   $\Omega$  cm. Optical transmission measurements between 0.6 and 1.2  $\mu\text{m}$  wavelength on the latter films revealed a finite imaginary part of the refractive index ( $n = 2.06 + i0.10$ ), indicating absorbing properties probably due to oxygen loss during deposition. All other  $\text{Ga}_2\text{O}_3$  films show no detectable absorption in our measurements between 0.6 and 1.2  $\mu\text{m}$  wavelength.

The voltage, at which destructive breakdown occurs, normalized to the film thickness, is defined as the breakdown field  $E_m$ . Figure 3 shows the dc breakdown field versus substrate temperature with  $\text{O}_2$  partial pressure as a parameter for films with thicknesses between 500 and 4000 Å. The best results ( $E_m = 2.1 \pm 0.12$  MV/cm) were again obtained for  $T_s = 40$  °C with no introduction of oxygen into the deposition chamber. The breakdown voltage scales with the oxide thickness for films thicker than 500 Å, however, slightly larger values for  $E_m$  were obtained for thinner films. We attribute the degradation of dielectric properties such as breakdown field (Fig. 3) and specific resistivity (Fig. 2) at higher substrate temperatures to oxygen loss during deposition.

Capacitance measurements were done on  $\text{Ga}_2\text{O}_3$  layers deposited under two different conditions (i)  $T_s = 40$  °C, no additional  $\text{O}_2$  introduced, and (ii)  $T_s = 125$  °C,  $\text{O}_2$  partial pressure  $p_{\text{ox}} = 2 \times 10^{-4}$  Torr. The capacitance is found to be independent on frequency within the measurement range between 100 Hz and 1 MHz and scales correctly with oxide thickness. The static dielectric constant  $\epsilon_s$  was determined to be  $9.93 \pm 0.39$  and  $10.2 \pm 0.6$ , respectively. These results are in close agreement with  $\epsilon_s = 10.2 \pm 0.3$  for single-crystal  $\text{Ga}_2\text{O}_3$  platelets.<sup>8</sup>

Figure 4 shows the current versus  $\sqrt{\text{electric field}}$  characteristics of a Ti- $\text{Ga}_2\text{O}_3$ -GaAs MIS structure with a 864 Å thick oxide layer deposited at 40 °C with no  $\text{O}_2$  intentionally introduced into the chamber. Two distinct regions of current transport can be clearly identified. The ohmic  $I$ - $V$  characteristic at low fields is due to hopping of thermally excited electrons from one isolated state in the oxide to another.<sup>10</sup> As shown in the inset of Fig. 4, the current at high fields is dominated by field enhanced thermal excitation of trapped

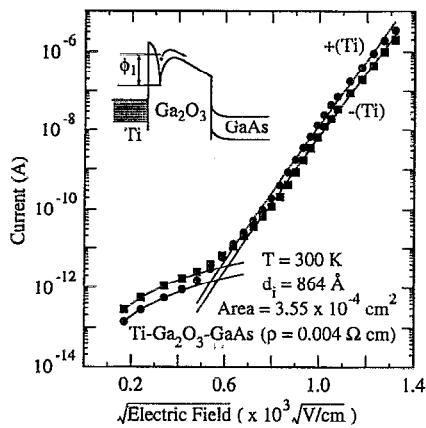


FIG. 4. Current- $\sqrt{\text{electric field}}$  characteristic of a Ti-Ga<sub>2</sub>O<sub>3</sub>-GaAs metal-insulator-semiconductor structure with an 864 Å thick oxide layer deposited at 40 °C with no O<sub>2</sub> intentionally introduced into the deposition chamber. The characteristics, which are nearly independent of the polarity of the electrodes, show two distinct regions of ohmic and Frenkel-Poole current transport mechanisms. The inset shows Frenkel-Poole emission from trapped electrons.

electrons into the conduction band (internal Schottky emission or Frenkel-Poole effect)

$$j \propto E \exp(-q\{\phi_1 - (qE/\pi\epsilon_0\epsilon_d)^{0.5}\}/kT\},$$

where  $E$  is the electric field,  $q$  the electronic charge,  $\phi_1$  the barrier height,  $\epsilon_d$  the dynamic dielectric constant,  $T$  the temperature in  $K$ , and  $k$  the Boltzmann constant. The Frenkel-Poole emission is considered as a bulk effect in the insulating layer with a dynamic dielectric constant  $\epsilon_d$  between  $\epsilon_\infty=3.61$  (Ref. 2) and  $\epsilon_s=9.93$ . From the high field characteristics in Fig. 4, we found a dynamic dielectric constant  $\epsilon_d$  of 4. This is in agreement with the assumption of Frenkel-Poole emission as the dominant transport mechanism. On the other hand, assuming Schottky emission across the metal-insulator or insulator-semiconductor interface as the dominant trans-

port mechanism would lead to an anomalous dynamic dielectric constant  $\epsilon_d < 1$ .<sup>11</sup> Thus, like in other dielectrics,<sup>10</sup> the current transport mechanisms at both low and high electric fields were found to be bulk rather than electrode controlled.

In summary, we have demonstrated that high quality, dielectric Ga<sub>2</sub>O<sub>3</sub> thin films can be deposited by electron-beam evaporation using a single-crystal high purity Gd<sub>3</sub>Ga<sub>5</sub>O<sub>12</sub> source. Excellent dielectric properties for as-deposited films were obtained at substrate temperatures of 40 °C with no excess oxygen and at 125 °C with an oxygen partial pressure of  $2 \times 10^{-4}$  Torr. We measured specific resistivities  $\rho$  and dc breakdown fields  $E_m$  of up to  $6 \times 10^{13}$  Ω cm and 2.1 MV/cm, respectively. Static dielectric constants between 9.93 and 10.2 were determined for these films. The current transport mechanisms in MIS and MIM structures were found to be bulk controlled rather than electrode controlled.

We are very grateful to H. S. Luftman for performing the SIMS measurements and for helpful discussions. We wish to thank R. L. Masaitis for performing the Auger spectroscopy measurements.

- <sup>1</sup>A. Callegari, P. D. Hoh, D. A. Buchanan, and D. Lacey, *Appl. Phys. Lett.* **54**, 332 (1989).
- <sup>2</sup>M. Passlack, N. E. J. Hunt, E. F. Schubert, G. J. Zydzik, W. S. Hobson, M. Hong, J. P. Mannaerts, C. G. Bethea, J. Lopata, and J. D. Wynn (unpublished).
- <sup>3</sup>M. Fleischer, W. Hanrieder, and H. Meixner, *Thin Solid Films* **190**, 93 (1990).
- <sup>4</sup>S. Adachi, *J. Appl. Phys.* **58**, R1 (1985).
- <sup>5</sup>*CRC Handbook of Chemistry and Physics 1989-1990* (CRC, Boca Raton, FL, 1989).
- <sup>6</sup>T. M. Terman, *Solid-State Electron.* **5**, 285 (1962).
- <sup>7</sup>E. S. Aydil, K. P. Giapis, R. A. Gottscho, V. M. Donnelly, and E. Yoon, *J. Vac. Sci. Technol. B* **11**, 195 (1993).
- <sup>8</sup>See, for example, B. Hoeneisen, C. A. Mead, and M.-A. Nicolet, *Solid-State Electron.* **14**, 1059 (1971).
- <sup>9</sup>L. G. van Uitert and S. Singh (unpublished).
- <sup>10</sup>S. M. Sze, *J. Appl. Phys.* **38**, 2951 (1967).
- <sup>11</sup>S. M. Sze, *Physics of Semiconductor Devices* (Wiley, New York, 1981), p. 403.